Steady-State and Pre-Steady-State Kinetic Analysis of *Mycobacterium tuberculosis* Pantothenate Synthetase†

Renjian Zheng and John S. Blanchard*

Department of Biochemistry, Albert Einstein College of Medicine, 1300 Morris Park Avenue, Bronx, New York 10461

Received July 20, 2001

ABSTRACT: Pantothenate synthetase (EC 6.3.2.1), encoded by the *panC* gene, catalyzes the essential ATP-dependent condensation of D-pantoate and β-alanine to form pantothenate in bacteria, yeast and plants. Pantothenate synthetase from *Mycobacterium tuberculosis* was expressed in *E. coli*, purified to homogeneity, and found to be a homodimer with a subunit molecular mass of 33 kDa. Initial velocity, product, and dead-end inhibition studies showed the kinetic mechanism of pantothenate synthetase to be Bi Uni Uni Bi Ping Pong, with ATP binding followed by D-pantoate binding, release of PP_i, binding of β-alanine, followed by the release of pantothenate and AMP. Michaelis constants were 0.13, 0.8, and 2.6 mM for D-pantoate, β-alanine, and ATP, respectively, and the turnover number, k_{cat}, was 3.4 s^{-1}. The formation of pantoyl adenylate, suggested as a key intermediate by the kinetic mechanism, was confirmed by ^{31}P NMR spectroscopy of [^{18}O]AMP produced from ^{18}O transfer using [*carboxyl*-^{18}O]pantoate. Single-turnover reactions for the formation of pyrophosphate and pantothenate were determined using rapid quench techniques, and indicated that the two half-reactions occurred with maximum rates of 1.3 ± 0.3 and 2.6 ± 0.3 s^{-1}, respectively, consistent with pantoyl adenylate being a kinetically competent intermediate in the pantothenate synthetase reaction. These data also suggest that both half-reactions are partially rate-limiting. Reverse isotope exchange of [^{14}C]-β-alanine into pantothenate in the presence of AMP was observed, indicating the reversible formation of the pantoyl adenylate intermediate from products.

Pantothenate is a B-group vitamin (vitamin B_5), and is the key precursor for the biosynthesis of coenzyme A (CoA) and acyl carrier protein (ACP) (*1*). Both microorganisms and plants must synthesize pantothenate, while mammals must obtain it from their diet (*1*). Both CoA and ACP are essential cofactors for cell growth and are involved in many metabolic reactions in crucial biosynthetic pathways (*2*). CoA and ACP fatty acyl thioesters are important intermediates in fatty acid biosynthesis (*2, 3*). The pantothenate biosynthetic pathway is best characterized in *Escherichia coli* and *Salmonella typhimurium* (Scheme 1). Pantothenate is synthesized from α-ketoisovalerate, an intermediate in valine and leucine biosynthesis, in three steps (*4, 5*). The genes encoding the enzymes involved in pantothenate biosynthesis from α-ketoisovalerate (*panB*, *panC*, *panD*, and *panE*) have been identified (*6, 7*). The biosynthesis of pantothenate is essential for the growth of *Mycobacterium tuberculosis* (Vasan, S. K., and Jacobs, W. R., Jr., personal communication), suggesting that the enzymes involved in pantothenate biosynthesis are appropriate targets for the development of antibacterial agents.

Pantothenate synthetase (EC 6.3.2.1), the product of the *panC* gene, catalyzes the synthesis of pantothenate from D-pantoate and β-alanine with the hydrolysis of ATP[1] into AMP and PP_i (*8*). Pantothenate synthetase has been purified and partially characterized from *E. coli*, *L. japonicus*, and *O. sativum* (*9, 10*). The enzyme exists as either a homotetramer (*E. coli*) or a dimer (*L. japonicus*). Mg^{2+} is essential for the pantothenate synthetase reaction (*8, 10*). The three-dimensional structure of *E. coli* pantothenate synthetase was reported very recently (*11*). The kinetic mechanism of the *E. coli* enzyme has been reported to be a Bi Uni Uni Bi Ping Pong mechanism, and the formation of an enzyme−pantoyl adenylate intermediate was suggested (*9*) (Scheme 2). Based on the kinetic mechanism, the overall reaction consists of two sequential steps: pantoyl adenylate formation, and the subsequent nucleophilic attack on the anhydride by β-alanine to form pantothenate (Schemes 3 and 4). The formation of an acyl adenylate in the mechanism of both malonyl-CoA synthetase and aminoacyl-tRNA synthetase has been documented (*12, 13*) (Scheme 5). Malonyl-CoA synthetase, a member of the acyl adenylate/thioester-forming enzyme family, catalyzes the formation of malonyl-CoA via activation of the carboxyl group of malonate with ATP to form a malonyl-AMP intermediate prior to transfer to CoA. Similarly, aminoacyl-tRNA synthetases catalyze the activation of the carboxyl group of amino acids with ATP to form the corresponding aminoacyl adenylate, and subsequent acyl transfer to the corresponding cognate tRNA. Malonyl-CoA

† This work was supported by NIH Grant AI33696.

* To whom correspondence should be addressed. Phone: (718) 430-3096; Fax: (718) 430-8565; E-mail: blanchar@aecom.yu.edu.

[1] Abbreviations: PS, pantothenate synthetase; HP, D-(−)-pantoate; Pan, pantothenate; NADH, reduced β-nicotinamide adenine dinucleotide; IPTG, isopropyl-1-thio-β-D-galactopyranoside; SDS−PAGE, sodium dodecyl sulfate−polyacrylamide gel electrophoresis; Hepes, 4-(2-hydroxyethyl)-1-piperazineethanesulfonic acid; TEA, triethanolamine; ATP, adenosine 5′-triphosphate; AMP-CPP, α,β-methyleneadenosine 5′-triphosphate; AMP, adenosine 5′-monophosphate; PEI-F TLC, poly(ethylenimine)cellulose-F thin-layer chromatography; EDTA, ethylenediaminetetraacetic acid; NMR, nuclear magnetic resonance.

10.1021/bi011522+ CCC: $20.00
Published on Web 10/06/2001

Scheme 1

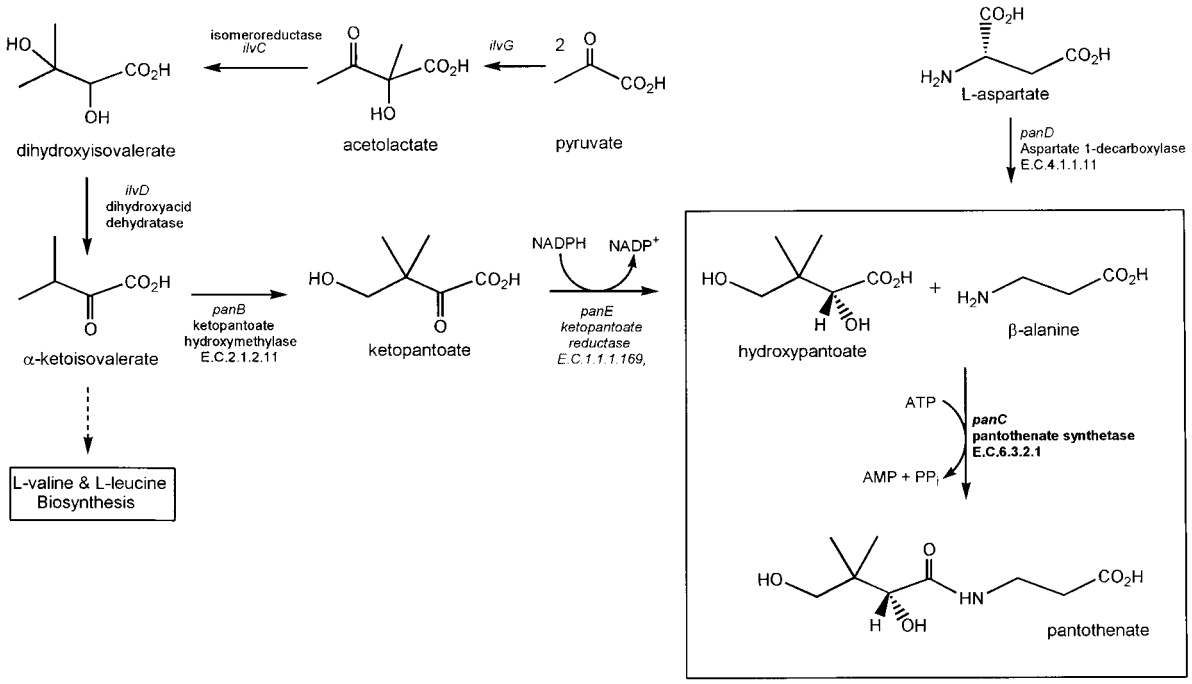

Scheme 2

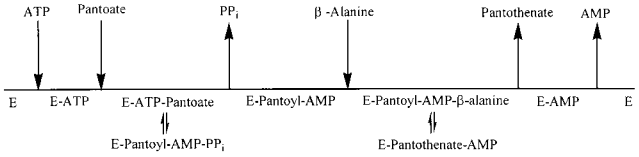

synthetase utilizes an ordered Bi Uni Uni Bi Ping Pong kinetic mechansm, whereas aminoacyl-tRNA synthetase show a great diversity in the steady-state kinetic mechanism (*14*, *15*).

In this study, we report the steady-state and pre-steady-state kinetic parameters and chemical mechanism of the *M. tuberculosis* pantothenate synthetase. These mechanistic studies, in combination with detailed structural studies of the enzyme in complexes with its substrates or products, may aid in the development of this essential pathway as a target for inhibitor design studies.

MATERIALS AND METHODS

Materials. NADH, IPTG, ATP, β-alanine, [^{14}C]-β-alanine, myokinase (rabbit muscle), pyruvate kinase (rabbit muscle), and lactate dehydrogenase (rabbit muscle) were purchased from Sigma. All restriction enzymes and T4 DNA ligase were obtained from New England Biolabs. *Pfu* DNA polymerase was from Stratagene. pET23a(+) plasmid and *E. coli* strain BL21(DE3) were obtained from Novagen. All chromatographic supports were from Pharmacia. PEI-F TLC plates were obtained from EM Science. [α-^{32}P]ATP (3000 Ci/mmol) and [γ-^{32}P]ATP (6000 Ci/mmol) were from NEN DuPont Corp. Pantoyl lactone and other chemicals were obtained from Aldrich.

Preparation of Pantoic Acid and [carboxyl-^{18}O]Pantoic Acid. Pantoic acid was prepared from pantoyl lactone using NaOH as previously described (*16*). [*carboxyl*-^{18}O]Pantoic acid was prepared by incubating pantoyl lactone with an equal molar amount of Na^{18}OH (10 μL of 10 N NaOH, 90

Scheme 3

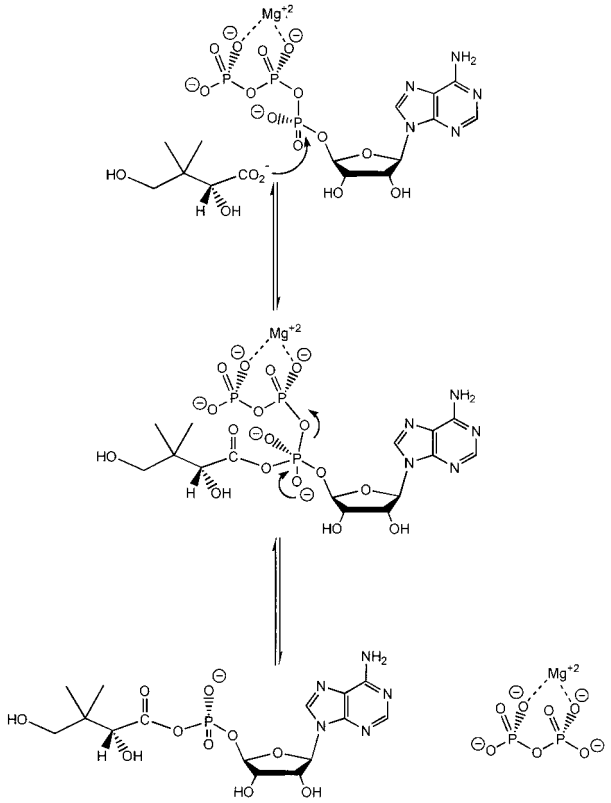

μL of 95% $H_2{}^{18}O$; final concentration of ^{18}O was 85.5%) for 2 h at room temperature, and then adjusting the pH to 7.0. ^{1}H NMR spectra of pantoic acid and [*carboxyl*-^{18}O]-pantoic acid are identical: (300 MHz, D_2O) δ 3.92 (s, 1H), 3.57 (dd, 2H), and 1.02 (d, 6H); ^{13}C NMR (300 MHz, D_2O) δ 180.17 (carbonyl-^{16}O), 180.14 (carbonyl-^{18}O), 77.95, 69.42, 38.58, 20.90, 20.08.

Cloning and Expression of M. tuberculosis Pantothenate Synthetase. The *panC* gene, encoding pantothenate syn-

Scheme 4

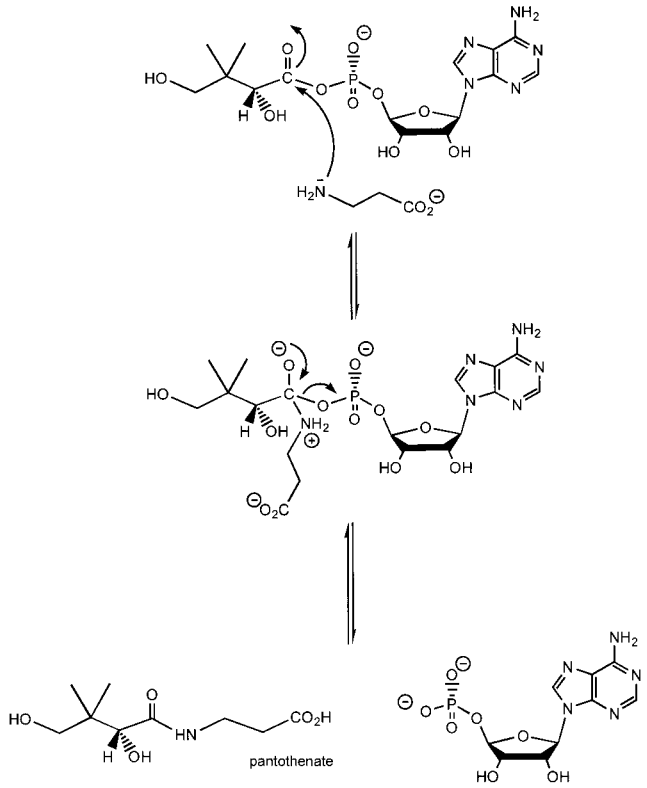

thetase, was obtained by PCR amplification of the gene (Rv3602c) from genomic DNA of *M. tuberculosis* using *Pfu* DNA polymerase and two primers (5′-ATTCCATATGAC-GATTCCTGCGTTCCATC-3′; 5′-CCAAGCTTTCAGTTTC-TCCAATGTGATTC-3′) containing *Nde*I and *Hin*dIII restriction sites, respectively. The PCR product was cloned into the PCR-Blunt vector (Invitrogen) and transformed into TOP 10 competent cells. After purification of the plasmid DNA from TOP 10 cells, the *panC* gene was cleaved with *Nde*I and *Hin*dIII restriction enzymes from the recombinant PCR-Blunt plasmid and ligated into an *Nde*I- and *Hin*dIII-digested pET23a(+) plasmid (Novagen). The resulting plasmid, pET23a(+):*panC*, was transformed into competent cells of *E. coli* strain BL21(DE3), and the cells were grown at 37 °C to an A_{600} of 0.6 in LB medium containing 50 μg/mL carbenicillin. IPTG was added to the culture (final concentration of IPTG = 0.5 mM), and growth was continued for an additional 4 h at 37 °C.

Purification and Analysis of the Recombinant Pantothenate Synthetase. Cells (12 g) were suspended in 50 mL of 40 mM TEA-HCl, pH 7.8, containing protease inhibitors (Boehringer Mannheim) and 20 μg/mL lysozyme. After sonication, cells debris was removed by centrifugation for 45 min at 11 000 rpm. Nucleic acids were precipitated by the addition of 1% streptomycin sulfate to the supernatant. After centrifugation for 45 min at 11 000 rpm, the supernatant was dialyzed against 20 mM TEA-HCl, pH 7.8. The supernatant was applied to a 5 × 35 cm Fast Flow Q-Sepharose anion-exchange column, and proteins were eluted with a linear 0−0.8 M NaCl gradient. Active fractions were pooled, concentrated to 4 mL, and loaded onto a 1.6 × 70 cm Superdex 200 gel filtration column. The enzyme was eluted at 0.5 mL/min, and the active fractions were pooled and applied to a 1 × 10 cm Mono Q high-resolution anion-exchange column to remove minor contaminating species.

Protein concentrations were measured using a Bio-Rad protein assay kit with bovine serum albumin as a standard. The subunit molecular weight of pantothenate synthetase was determined by SDS−polyacrylamide gel electrophoresis according to the method of Laemmli (*17*). The native molecular weight was estimated by using a Superdex 200 gel filtration column calibrated using Bio-Rad molecular weight markers. Electrospray ionization/mass spectrometry was performed on the purified enzyme to determine the subunit molecular mass of pantothenate synthetase. N-terminal sequencing of the purified recombinant pantothenate synthetase was performed with an Applied Biosystems sequencer using standard Edman chemistry.

Steady-State Kinetics. Pantothenate synthetase activity was assayed spectrophotometrically by coupling the formation of AMP to the reactions of myokinase, pyruvate kinase, and lactate dehydrogenase as described previously (*18*). The decrease in absorbance of NADH at 340 nm (ϵ_{340} = 6220 M^{-1} cm^{-1}) was measured at 25 °C using a UVIKON 943 spectrophotometer with a circulating water bath and thermospacers. The standard reaction contained 100 mM Hepes, pH 7.8, 10 mM $MgCI_2$, 10 mM ATP, 5 mM β-alanine, 5 mM D-pantoate, 1 mM potassium phosphoenolpyruvate, 200 μM NADH, 18 units of myokinase, 18 units of pyruvate kinase, and 18 units of lactate dehydrogenase in a total volume of 1.0 mL at 25 °C. After incubation for 5 min at 25 °C, reactions were initiated by the addition of pantothenate

Scheme 5

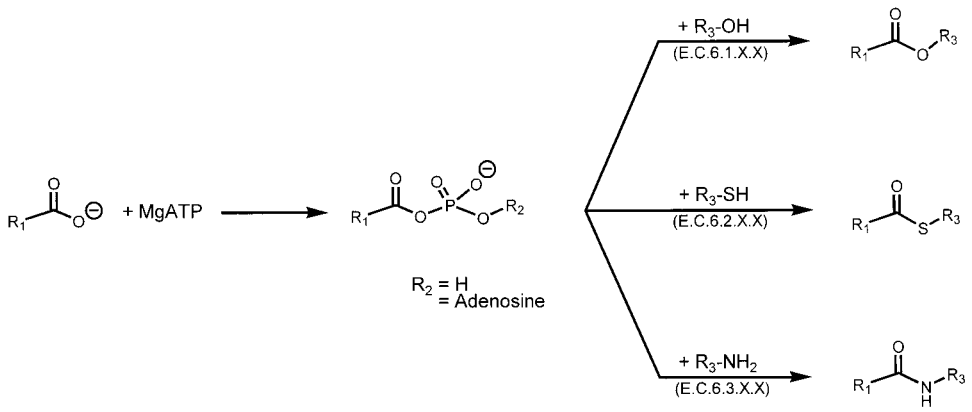

Scheme 6

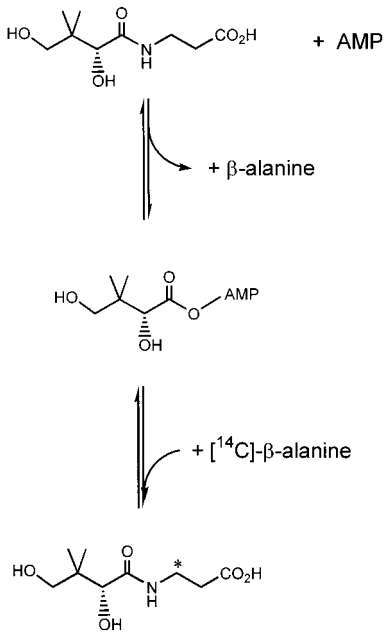

synthetase ($\leq$10 μL). PS enzyme activities were corrected for background activity. The rate of pantothenate formation is proportional to the rate of NADH oxidation where two molecules of NADH are oxidized for each molecule of pantothenate formed.

Initial velocity experiments were carried out at various concentrations of one substrate in the presence of different fixed levels of a second substrate and with the concentration of the third substrate kept saturating and constant. Product inhibition studies were carried out at various substrate concentrations in the presence or absence of the products, pantothenate and AMPCPP (an analogue of ATP). Enzyme specificity for analogues of β-alanine was examined using the same kinetic assay, substituting analogues for β-alanine.

Effects of Metal Ions on Enzyme Activity. Effects of divalent cation (Mg^{2+}, Mn^{2+}, Co^{2+}, Ni^{2+}, Zn^{2+}, and Cu^{2+}) on PS enzyme activity were determined by an isotopic method using [α-^{32}P]ATP since the coupling enzyme activities are also metal-dependent. Reaction mixtures contained 10 mM [α-^{32}P]ATP (30 μCi/μmol), 5 mM sodium pantoate, 5 mM β-alanine, 0.1−20 mM metal ion in 100 mM Hepes, pH 7.8. The reaction was initiated by the addition of pantothenate synthetase ($\leq$10 μL). After incubation for 3 min at 25 °C, the reaction was stopped by the addition of 300 mM EDTA, and by heating reaction mixtures in a boiling water bath for 1 min, and pelleting precipited enzyme by centrifugation. The supernatant was spotted onto PEI TLC plates, and radiolabeled ATP and AMP were separated using 0.9 M LiCl as the mobile phase. The amount of AMP formed was quantitated using a Phosphorimager (Molecular Dynamics) and corrected for nonenzymatic activity.

Pre-Steady-State Kinetics. Single-turnover experiments were performed at 25 °C using a KinTek rapid quench flow apparatus (model RQF-3) equipped with a constant temperature circulating water bath. The first half-reaction (pyrophosphate formation) was initiated by rapidly mixing 20 μL of 56 μM PS enzyme containing 10 mM sodium pantoate in 100 mM Hepes, pH 7.8, with 20 μL of a solution containing 80−1600 μM [γ-^{32}P]ATP (20 μCi/μmol), 20 mM $MgCl_2$ in100 mM Hepes, pH 7.8. Control reactions excluded pantoate or PS enzyme from the reaction above. The reaction was incubated for a given time interval and then quenched with 152 μL of 100 mM EDTA. The enzyme was denatured by heat treatment in a boiling water bath for 1 min after quenching. After centrifugation, aliquots of the reaction were spotted onto PEI TLC plates, and radiolabeled ATP and pyrophosphate were resolved using 0.9 M guanidine hydrochloride as the mobile phase.

The rate of the second half-reaction (pantothenate formation) was determined as follows. Twenty microliters containing 60 μM PS enzyme, 20 mM $MgCl_2$, 20 mM ATP, 10 mM sodium pantoate in 100 mM Hepes, pH 7.8, was preincubated at 25 °C for 5 min to allow complete formation of the pantoyl adenylate intermediate, followed by rapid mixing with 20 μL of 100−2000 μM [^{14}C]-β-alanine (50 μCi/μmol) in 100 mM Hepes, pH 7.8, and 100 mM EDTA. Control reactions excluded pantoate or enzyme from the reaction above. The reaction was incubated for a given time interval and then quenched with 152 μL of 0.1 N HCl. The acid-quenched solution was heated in a boiling water bath for 1 min and centrifuged to pellet denatured protein. The solution was spotted onto PEI TLC plates, and [^{14}C]-β-alanine and [^{14}C]pantothenate were separated using 0.4 M formic acid as a developing solvent. Both pyrophosphate and pantothenate were quantitated using a Phosphorimager (Molecular Dynamics) and corrected for nonenzymatic activity.

^{18}O Transfer. Reaction mixtures contained 10 mM $MgCl_2$, 10 mM ATP, 10 mM β-alanine, 15 mM [*carboxyl*-^{18}O]-pantoate, and 5 μg of pantothenate synthetase in 0.5 mL of 25 mM Hepes, pH 8.0. After incubation for 2 h at 37 °C, the solution was filtered through a YM 10 Amicon membrane to remove the enzyme. Then 0.12 mL of D_2O was added to the solution (final concentration of D_2O = 20%). Control experiments were performed in the same manner as described above except using unlabeled pantoate in the reaction. After the pH was adjusted to 8.6, the solution was analyzed by ^{31}P NMR on a Bruker AMX300 NMR spectrometer operating at a frequency of 121 MHz.

Reverse Isotope Exchange. Reverse isotope exchange reactions contained either 0 or 10 mM AMP, 1, 10, or 100 mM pantothenate, 0.5 mM [^{14}C]-β-alanine (50 μCi/μmol), and 15 μM pantothenate synthetase in 100 mM Hepes, pH 7.8. Control reactions omitted pantothenate or enzyme from the reaction mixture above. The exchange and control reactions were incubated at 25 °C with 4 μL aliquots removed at the designated time points. The reaction was stopped by adding 16 μL of 0.1 N HCl and then heated in a boiling water bath for 1 min. After centrifugation, the solution was spotted onto PEI TLC plates, and [^{14}C]-β-alanine and [^{14}C]pantothenate were separated using 0.4 M formic acid as a developing solvent. The amount of pantothenate formed was quantitated using a phosphorimager (Molecular Dynamics) and corrected for nonenzymatic activity.

Data Analysis. Kinetic data were fitted to the appropriate rate equations by using the programs developed by Cleland (*19*). Initial velocity data were fitted to eq 1 for a parallel pattern and to eq 2 for an intersecting pattern. Inhibition data

were fitted to eqs 3−5 for competitive, uncompetitive, and noncompetitive inhibition patterns, respectively.

$$v = VAB/(K_aB + K_bA + AB) \quad (1)$$

$$v = VAB/(K_{ia}K_b + K_aB + K_bA + AB) \quad (2)$$

$$v = VA/[K(1 + I/K_{is}) + A] \quad (3)$$

$$v = VA/[K + A(1 + I/K_{ii})] \quad (4)$$

$$v = VA/[K(1 + I/K_{is}) + A(1 + I/K_{ii})] \quad (5)$$

Single-turnover progress curve data were fitted to eq 6 (20):

$$Y = A(1 - e^{-k_{obs}t}) \quad (6)$$

For a two-step binding mechanism, the dependence of the single-exponential rate constant, k_{obs}, as a function of substrate concentration is given by eq 7 (*21*). For both half-reactions in pantothenate synthetase, the intercept of k_{obs} versus substrate concentration curves appeared to be approximately zero (Figures 2B and 3B). The data were thus fitted to eq 8, where $k_{off} = 0$.

$$k_{obs} = k_{max}[S]/(K_d + [S]) + k_{off} \quad (7)$$

$$k_{obs} = k_{max}[S]/(K_d + [S]) \quad (8)$$

Data for reverse isotope exchange were fitted to eq 9 (*22*):

$$v = -\{[A][P]/([A] + [P])\}(1/t)\ln(1 - F) \quad (9)$$

where [A] = β-alanine concentration, [P] = pantothenate concentration, and F = the fraction of equilibrium value obtained at time t. Plots of $\ln(1 - F)$ versus t were linear to isotopic equilibrium, and the slopes were used to determined the velocity.

RESULTS

Purification and Properties of the Recombinant Pantothenate Synthetase. M. tuberculosis pantothenate synthetase was purified to homogeneity in a yield of 181 mg from 12 g of *E. coli* cells by using consecutive Fast Flow Q-Sepharose anion-exchange, Superdex 200 gel filtration, and Mono Q high-resolution anion-exchange column chromatography. Protein concentrations were determined using a Bio-Rad protein assay kit using bovine serum albumin as a standard. The subunit molecular mass of pantothenate synthetase determined by SDS−polyacrylamide gel electrophoresis is 33 kDa, consistent with the molecular weight of 32 677 calculated from the amino acid sequence of the *M. tuberculosis* enzyme. A Superdex 200 gel filtration column calibrated using Bio-Rad molecular weight markers was used to estimate the molecular weight of the native enzyme as 65 000, suggesting the native enzyme exists as a dimer. N-terminal sequencing of the recombinant, homogeneous enzyme resulted in an N-terminal peptide sequence of TIPAFHPGEL, consistent with the predicted amino acid sequence lacking the initiating methionine residue. Electrospray ionization/mass spectrometry analysis demonstrated that the enzyme subunit has a molecular mass of 32 545 Da, consistent with a molecular mass of 32 546 Da calculated from the protein sequence minus the N-terminal methionine.

Table 1: Kinetic Parameters of *M. tuberculosis* Pantothenate Synthetase

substrate	K_m (mM)	k_{cat} (s^{-1})	k_{cat}/K_m ($M^{-1}\,s^{-1}$)
D-pantoate	0.13 ± 0.03	3.4 ± 0.2	2.6×10^4
β-alanine	0.8 ± 0.1		4.3×10^3
ATP	2.6 ± 0.4		1.3×10^3

Steady-State Kinetic Studies. The kinetic mechanism of *M. tuberculosis* pantothenate synthetase was determined by initial velocity experiments using the coupled enzyme assay described above. The parallel lines revealed in double reciprocal plots of the initial velocity using either ATP or pantoate and β-alanine suggested a Ping Pong kinetic mechanism for pantothenate synthetase. The data were fitted to eq 1 or 2, yielding K_m values for the three substrates: 0.13 mM for pantoate, 0.8 mM for β-alanine, and 2.6 mM for ATP, and a k_{cat} of 3.4 s^{-1} (Table 1). Product and dead-end inhibition studies were carried out at various substrate concentrations in the presence or absence of the product, pantothenate, and the dead-end inhibitor, AMPCPP (a nonhydrolyzable analogue of ATP). Pantothenate exhibited uncompetitive inhibition versus both D-pantoate and ATP, and noncompetitive inhibition versus β-alanine. AMP-CPP exhibited competitive inhibition versus ATP, uncompetitive inhibition versus β-alanine, and noncompetitive inhibition versus D-pantoate (Table 2). These data are completely consistent with a Bi Uni Uni Bi Ping Pong kinetic mechanism for the pantothenate synthetase reaction. The substrate specificity of the enzyme for analogues of β-alanine is shown in Table 3.

Effects of Metal Ions on Enzyme Activity. The ability of various divalent metal ions to promote pantothenate synthetase activity is shown in Figure 1. Pantothenate synthetase was most active in the presence of 10 mM Mg^{2+} or Mn^{2+}, exhibiting modest activity in the presence of Co^{2+}, Ni^{2+}, or Zn^{2+} and no activity with Cu^{2+}.

Pre-Steady-State Kinetic Analysis. The rate of pyrophosphate formation in the first half-reaction was determined by single-turnover experiments using rapid quench flow techniques with [γ-^{32}P]ATP, in the absence of β-alanine. Plots of pyrophosphate concentration versus time were obtained using different concentrations of [γ-^{32}P]ATP (Figure 2A). The data were fitted to eq 6 to obtain the rate constants at each [ATP]. The rate constant for each reaction was subsequently plotted as a function of [ATP] (Figure 2B). The data were fitted to eq 8 to obtain the maximum value for the rate constant, $k_{max} = 1.3 \pm 0.3\ s^{-1}$, and a K_d value for ATP of 1.8 ± 0.5 mM.

The rate of pantothenate formation in the second half-reaction was measured in a similar manner. Plots of [pantothenate] formed versus time were generated using different concentrations of [^{14}C]-β-alanine (Figure 3A). The data were fitted to eq 6 to obtain the rate constant at each [β-alanine]. The rate of each reaction was subsequently plotted as a function of [β-alanine] (Figure 3B). The data were fitted to eq 8 to obtain the maximum value for the rate constant, $k_{max} = 2.6 \pm 0.3\ s^{-1}$, and a K_d value for β-alanine of 0.7 ± 0.1 mM.

Evidence for Pantoyl Adenylate Formation. The formation of the pantoyl adenylate intermediate was confirmed by ^{18}O transfer from [*carboxyl*-^{18}O]pantoate to AMP in the reaction catalyzed by pantothenate synthetase. The ^{13}C NMR spectra

Table 2: Product and Dead-End Inhibition of *M. tuberculosis* Pantothenate Synthetase

varied substrate	product inhibitor	K_{is} (mM)	K_{ii} (mM)	fixed substrate (mM)	inhibition pattern
β-alanine	pantothenate	13.5 ± 4.9	4.5 ± 1.7	ATP (10) D-pantoate (5)	NC
D-pantoate	pantothenate		5.7 ± 0.8	ATP (10) β-alanine (5)	UC
ATP	pantothenate		7.6 ± 1.1	D-pantoate (5) β-alanine (5)	UC
β-alanine	AMP-CPP[a]		0.42 ± 0.05	ATP (0.5) D-pantoate (5)	UC
D-pantoate	AMP-CPP	0.23 ± 0.10	0.36 ± 0.05	ATP (0.5) β-alanine (5)	NC
ATP	AMP-CPP	0.29 ± 0.03		D-pantoate (5) β-alanine (5)	C

[a] α,β-Methyleneadenosine 5′-triphosphate.

Table 3: Kinetic Parameters of β-Alanine Analogues for *M. tuberculosis* Pantothenate Synthetase

substrate analogue	K_m (mM)	k_{cat} (s^{-1})	k_{cat}/K_m ($M^{-1}\,s^{-1}$)
β-alanine	0.8 ± 0.1	3.4 ± 0.2	4.3×10^3
2-mercaptoethylamine	25.4 ± 2.5	0.063 ± 0.002	2.52
taurine	103 ± 39	0.19 ± 0.04	1.85
carbamate	36 ± 13	0.035 ± 0.0005	0.97
γ-aminobutyrate	335 ± 173	0.27 ± 0.06	0.81
glycine	84 ± 37	0.05 ± 0.01	0.6
γ-amino-β-hydroxybutyrate	580 ± 290	0.26 ± 0.09	0.45
5-aminovalerate	72 ± 17	0.03 ± 0.003	0.42
glycolate	108 ± 49	0.04 ± 0.01	0.38
ethylamine	93 ± 40	0.025 ± 0.0005	0.27
methylamine	79 ± 19	0.015 ± 0.0005	0.19

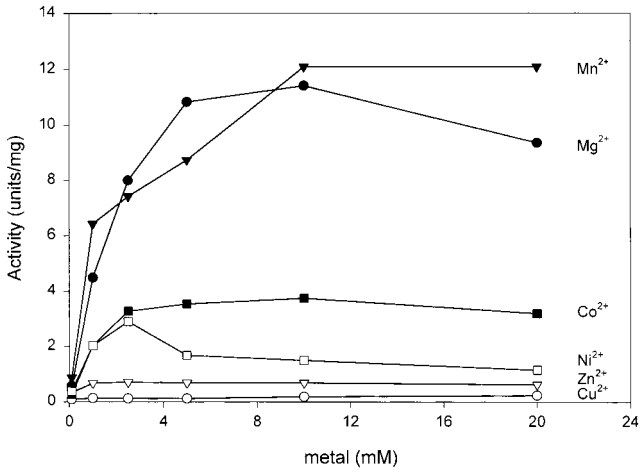

FIGURE 1: Effect of added divalent metal ions on pantothenate synthetase activity. Enzyme activities upon the addition of Mg^{2+} (●), Mn^{2+} (▼), Co^{2+} (■), Ni^{2+} (□), Zn^{2+} (▽), and Cu^{2+} (○) were measured by an isotopic method using [α-^{32}P]ATP. Details are given under Materials and Methods.

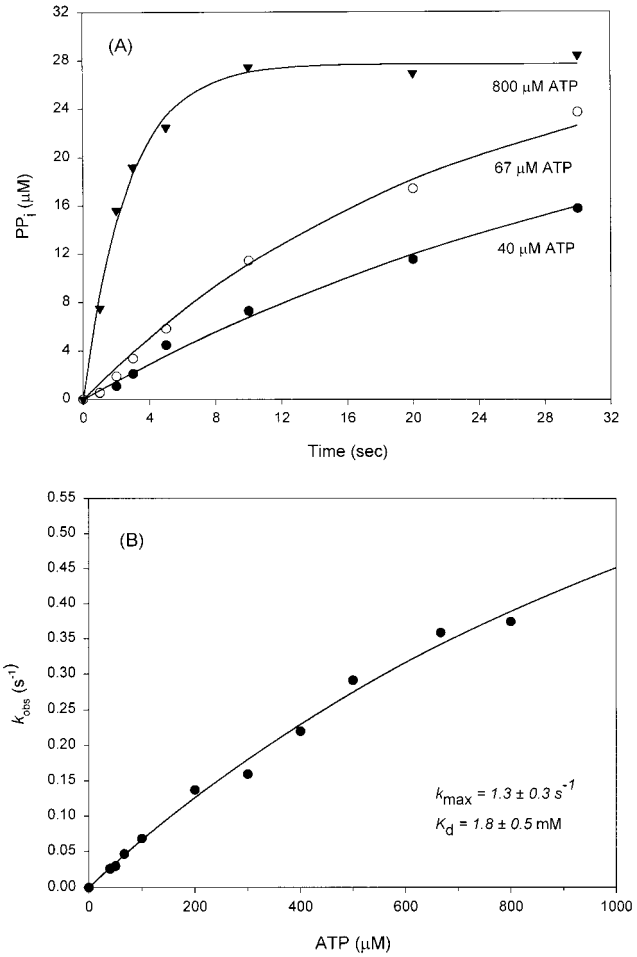

FIGURE 2: Pre-steady-state kinetics of pyrophosphate formation in the first half-reaction of *M. tuberculosis* pantothenate synthetase. (A) Single-turnover time courses for pyrophosphate formation. The curves are fits of the experimental data to eq 6, at representative ATP concentrations of 40, 67, and 800 μM. (B) Plot of the determined rate constants as a function of the ATP concentration. The data were fit to eq 8.

of [*carboxyl*-^{18}O]pantoate, prepared by the hydrolysis of pantoyl lactone with Na^{18}OH, revealed approximately 61% ^{18}O content in the two oxygens of the carboxyl group (Figure 4a). ^{18}O atom transfer from [*carboxyl*-^{18}O]pantoate to AMP was monitored by ^{31}P NMR spectroscopy. As shown in Figure 4c, two resonance peaks with a chemical shift difference of 0.024 ppm were observed corresponding to AMP labeled with no and one ^{18}O atom. The ^{18}O content of AMP was approximately 34% by ^{31}P NMR spectroscopy, as expected for transfer from one of the two equivalent carboxylate oxygens of pantoate. The ^{31}P NMR spectra of the AMP product in the control reaction, using unlabeled pantoate, exhibited a single resonance peak corresponding to unlabeled AMP (Figure 4b). These results indicated that a covalent pantoyl adenylate intermediate was formed during the pantothenate synthetase catalysis.

Reverse Isotope Exchange. The reversibility of the pantothenate synthetase partial reaction was determined using reverse isotope exchange. If reversible formation of the pantoyl adenylate intermediate could occur in the presence of AMP, pantothenate, and enzyme, the enzyme-bound

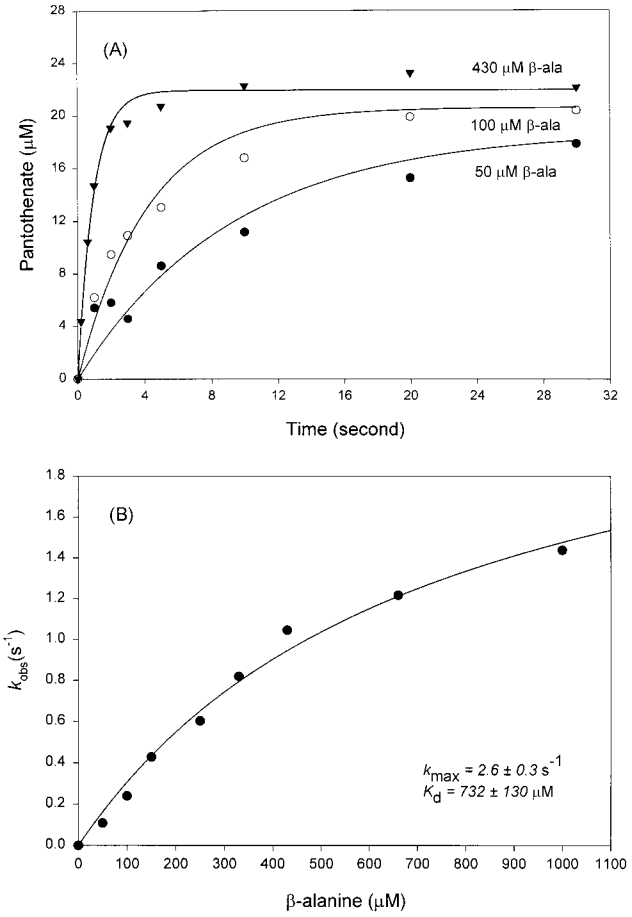

FIGURE 3: Pre-steady-state kinetics of pantothenate formation in the second half-reaction of *M. tuberculosis* pantothenate synthetase. (A) Single-turnover time courses for pantothenate formation. The curves are fits of the experimental data to eq 6, at representative β-alanine concentrations of 50, 100, and 430 μM. (B) Plot of the determined rate constants as a function of the β-alanine concentration. The data were fit to eq 8.

pantoyl adenylate intermediate could react with added [^{14}C]-β-alanine to form radiolabeled pantothenate (Scheme 6). The exchange of [^{14}C]-β-alanine into pantothenate was detected in this partial reaction. Figure 5 shows the time-dependent accumulation of radiolabeled pantothenate and the rates of isotope exchange at different concentrations of pantothenate. In the absence of AMP, negligible isotope exchange was observed. The exchange reaction proceeded to isotopic equilibrium over the course of 20 h. The reverse isotope exchange rate at saturating concentrations of pantothenate and AMP, and 0.5 mM [^{14}C]-β-alanine, was 4.4×10^{-3} min^{-1}.

DISCUSSION

The pantothenate biosynthetic pathway is essential for the biosynthesis of CoA and acyl carrier protein (ACP) in bacteria, yeast, and plants (*1*). Pantothenate is synthesized in three enzymatic steps from ketoisovalerate, which is also an intermediate in the biosynthesis of valine and leucine (*1*) (Scheme 1). The first unique step is catalyzed by the *panB*-encoded ketopantoate hydroxymethyltransferase using ketoisovalerate to generate ketopantoate, which is subsequently reduced to pantoate by the *panE*-encoded ketopantoate reductase. The *panC*-encoded pantothenate synthetase catalyzes the ATP-dependent condensation of pantoate with

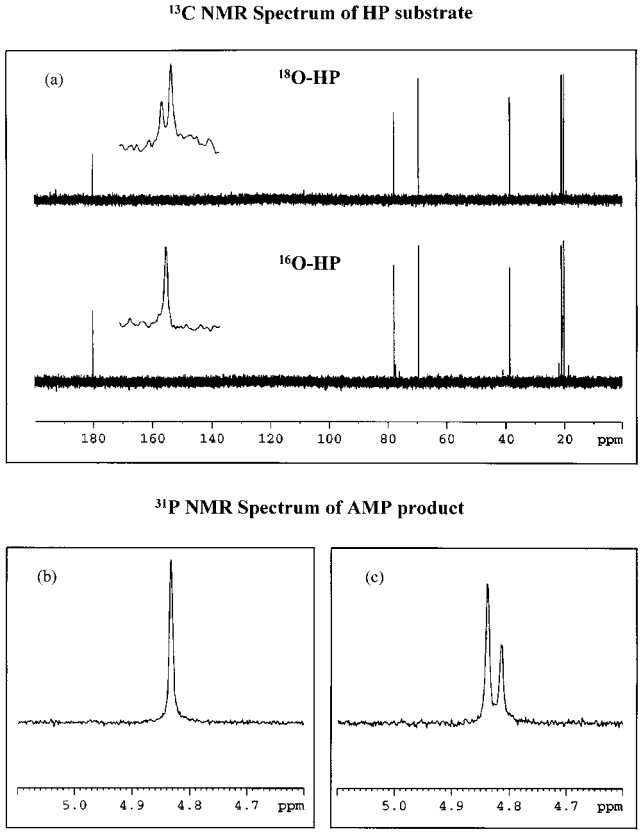

FIGURE 4: (a) Proton-decoupled ^{13}C NMR spectrum of pantoate prepared from pantoyl lactone using Na^{18}OH (85.5% ^{18}O, top panel) or NaOH (bottom panel). (b) ^{31}P NMR spectrum of AMP produced by the pantothenate synthetase reaction using [^{16}O]pantoate. (c) ^{31}P NMR spectrum of AMP produced by the pantothenate synthetase reaction using [^{18}O]pantoate. Reaction conditions are given under Materials and Methods.

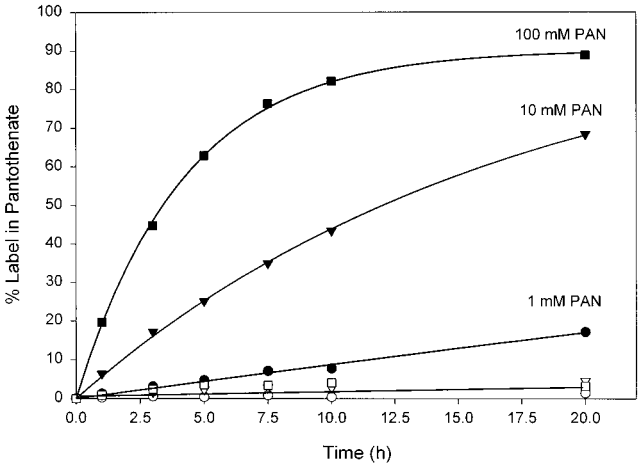

FIGURE 5: Reverse isotope exchange using 15 μM *M. tuberculosis* pantothenate synthetase, 0.5 mM [^{14}C]-β-alanine, 1 (●), 10 (▼), or 100 (■) mM pantothenate in the presence of 10 mM AMP, and 1 (○), 10 (▽), or 100 (□) mM pantothenate in the absence of AMP. Details are given under Materials and Methods.

β-alanine, generated by the *panD*-encoded aspartate 1-decarboxylase, to form pantothenate. The formation of pantothenate catalyzed by the synthetase is thought to proceed via activation of the carboxyl group of pantoate with ATP to form a pantoyl adenylate intermediate and then transfer of the pantoyl moiety to β-alanine. Since the *panC* gene is essential for the growth of *Mycobacterium tuberculosis*

(Vasan, S. K., and Jacobs, W. R., Jr., personal communication), the characterization of the mechanism of the *panC*-encoded enzyme is the first step in inhibitor design.

Steady-State Kinetic Mechanism. Initial velocity, product, and dead-end inhibition patterns for the *M. tuberculosis* pantothenate synthetase were in agreement with the Bi Uni Uni Bi Ping Pong kinetic mechanism reported for the *E. coli* pantothenate synthetase (*9*). Based on this kinetic mechanism, the reaction comprises two half-reactions: formation of the enzyme-bound pantoyl adenylate from ATP and pantoate; followed by pantoyl transfer to β-alanine to form pantothenate. The Bi Uni Uni Bi Ping Pong mechanism involving acyl adenylate intermediate formation has been documented for other ATP-dependent synthetases, including malonyl-CoA synthetase (*12*), fatty acyl-CoA synthetase (*23*), and some aminoacyl-tRNA synthetases (*13*). Malonyl-CoA synthetase has been shown to use a Bi Uni Uni Bi Ping Pong kinetic mechanism, consisting of an adenylation step followed by a thioesterification step. Although aminoacyl-tRNA synthetase-catalyzed reactions similarly involved acyl adenylate formation, different kinetic mechanisms have been claimed for different enzymes (*13*). For example, the Bi Uni Uni Bi Ping Pong kinetic mechanism was proposed for *E. coli* proline- and rat liver threonine-tRNA synthetases (*24*, *25*), while *E. coli* and yeast arginyl-tRNA synthetases were reported to use a sequential mechanism (*14*, *26*).

Metal ions are essential for the activity of pantothenate synthetase (*8*). We compared the effects of various divalent cations on *M. tuberculosis* pantothenate synthetase activity, and found that the enzyme was most active with Mg^{2+} or Mn^{2+} ions, consistent with metal ion specificity studies reported for the *E. coli* enzyme (*9*). We also examined analogues of β-alanine as substrates for the enzyme. As shown in Table 3, all analogues are poor substrates for the *M. tuberculosis* enzyme, exhibiting higher K_m and lower k_{cat} values. For example, the k_{cat}/K_m value for taurine is 2300-fold lower than that for β-alanine, suggesting the carboxyl group of β-alanine is important for the substrate specificity of the enzyme. γ-Aminobutyrate, which is only one carbon atom longer than β-alanine, exhibited a 5300-fold lower k_{cat}/K_m value than that of β-alanine, suggesting that the size of the substrate is important for binding to the enzyme.

Evidence for Pantoyl Adenylate Formation. Pantoyl adenylate has been proposed as an intermediate in the mechanism of the *E. coli* pantothenate synthetase (*9*). The steady-state kinetic mechanism determined in this study for the *M. tuberculosis* enzyme suggests a Ping Pong kinetic mechanism involving an enzyme−pantoyl adenylate intermediate. To probe the formation of a pantoyl adenylate intermediate in the pantothenate synthetase reaction, an ^{18}O transfer experiment was performed. In this reaction, [*carboxyl*-^{18}O]-labeled pantoate will interact with ATP to form [*carboxyl*-^{18}O]-pantoyl adenylate, followed by the transfer of the pantoyl moiety to β-alanine to generate pantothenate and [α-P $^{18}O_1$ $^{16}O_3$] AMP. The transfer of ^{18}O from [*carboxyl*-^{18}O]pantoate to AMP was demonstrated by ^{31}P NMR spectroscopy of the AMP product. Substitution of ^{18}O for ^{16}O in phosphate and phosphate esters induces a 0.024 ppm upfield chemical shift in the ^{31}P resonance per 18-oxygen atom (*27*). As shown in Figure 4c, two peaks separated by 0.024 ppm were observed, corresponding to AMP labeled with one or no ^{18}O atoms. Peak integration revealed that ca. 34% of the AMP product contained a single ^{18}O atom compared with the ca. 61% ^{18}O content of the [*carboxyl*-^{18}O]pantoate determined by integration of ^{13}C NMR resonance (Figure 1A). Wieland (*28*) has reported that γ-*O*-benzyl- and γ-*O*-methyl-pantoyl adenylate, analogues of the pantoyl adenylate intermediate that cannot lactonize, reacted with pyrophosphate in the presence of *E. coli* pantothenate synthetase to form ATP, supporting the formation of pantoyl adenylate in the kinetic pathway. For the malonyl-CoA synthetase-catalyzed reaction, the formation of malonyl-AMP was directly demonstrated by TLC analysis of the first half-reaction using [α-^{32}P]ATP (*12*). We attempted to directly identify the pantoyl adenylate intermediate by TLC methods, but were unable to, presumably due to the rapid lactonization of the adenylate (*28*). In the case of tyrosyl-tRNA synthetase, the enzyme catalyzes the formation of a thermodynamically unstable tyrosyl adenylate, which is stabilized by numerous hydrogen-bonding interactions between active site residues and the tyrosyl adenylate (*29*). This hydrolytically unstable acyl adenylate has never been directly isolated.

Pre-Steady-State Kinetics. To prove the participation of a pantoyl adenylate as a kinetically competent intermediate, it is necessary to directly measure the rates of adenylate formation and compare that to the overall reaction of pantothenate synthesis in the steady-state. We performed single-turnover studies for both the first and the second half-reactions using rapid-quench techniques. In the first half-reaction, pantoate reacts with ATP to form pantoyl adenylate and pyrophosphate at the enzyme active site, in the absence of β-alanine. The [^{32}P]PP_i product and the [γ-^{32}P]ATP substrate were cleanly separated by TLC using 0.9 M guanidine hydrochloride as a mobile phase, and quantitated by phosphorimager analysis. We observed no pantoate-independent pyrophosphorolysis of ATP with pantothenate synthetase, similar to results obtained with the D-Ala-D-X ligases (*30*). The maximum rate constant of PP_i formation in the first half-reaction was 1.3 s^{-1} under the condition used, which is slightly lower than the rate constant of the overall reaction measured from steady-state kinetic experiments using the coupled assay (see Materials and Methods). However, this rate constant for PP_i formation, measured in the absence of β-alanine, may not be as high as that determined in the presence of β-alanine, because the binding of β-alanine to the enzyme could facilitate the rate of formation of pyrophosphate. Using 1 equiv of β-alanine in rapid quench experiments of the first half-reaction, the rate of PP_i formation increased 38% (Zheng and Blanchard, data not shown). In the case of argininosuccinate synthetase, the rate constant for the formation of citrulline adenylate intermediate in the presence of aspartate is 600 times faster than when aspartate is absent, indicating that the binding of aspartate to the enzyme significantly enhances the rate of formation of the citrulline adenylate intermediate (*31*). Thus, the rate of pyrophosphate formation that we report (1.3 s^{-1}) corresponds to the rate of pantoyl adenylate formation in the absence of β-alanine, but is likely to be higher in the presence of the β-alanine concentration used in the determination of the steady-state value of k_{cat} (3.4 s^{-1}). The enhancement of the rate of the first half-reaction by the concentration of β-alanine is under investigation.

To characterize the decomposition of pantoyl adenylate intermediates, we measured the formation of pantothenate in the second single-turnover step. In this reaction, ATP and pantoate were incubated with pantothenate synthetase for 5

min to allow the complete formation of pantoyl adenylate at the active site, followed by mixing with [^{14}C]-β-alanine and EDTA, added to prevent additional turnover of the first half-reaction after mixing with β-alanine. After incubation for a given time interval, the reaction was quenched by HCl. The maximum rate constant of pantothenate formation was 2.6 ± 0.3 s^{-1}, which is within experimental error of the overall k_{cat} (3.4 ± 0.2 s^{-1}) determined in steady-state kinetic experiments using the coupled assay. In the case of isoleucyl-tRNA synthetase, a comparison of the rate of the formation of isoleucyl-tRNA from Ile-AMP•enzyme complex with the overall rate of formation of the same product from isoleucine, ATP, and tRNA^{Ile} showed the rates to be essentially equivalent, consistent with the role of isoleucyl adenylate as the intermediate in tRNA acylation (*32*). In the pantothenate synthetase reaction, the rate of synthesis of pantothenate from the pantoyl adenylate in the second chemical step is close to the rate of the formation of pantothenate in the overall reaction, indicating that the pantoyl adenylate intermediate is a kinetically viable intermediate.

Reverse Isotope Exchange. To assess the reversibility of pantoyl adenylate formation in the pantothenate synthetase reaction, we performed an isotope exchange experiment using pantothenate, AMP, and [^{14}C]-β-alanine. In this study, AMP-dependent isotope exchange of [^{14}C]-β-alanine into pantothenate was observed. In the absence of AMP, negligible exchange was observed (Figure 5), indicating that the exchange reaction is dependent on AMP. Thus, radiolabeled pantothenate was synthesized via the AMP-dependent formation of pantoyladenylate from pantothenate and AMP, followed by reaction with [^{14}C]-β-alanine. The reverse isotope exchange rate for pantothenate synthetase is very slow and equal to 4.4×10^{-3} min^{-1}, similar to the rate of reverse exchange observed for D-alanyl-D-alanine ligase, 5.9×10^{-3} min^{-1} (*33*). Pantothenate synthetase thus catalyzes the AMP-dependent hydrolysis of the peptide bond of pantothenate, a reaction that has few precedents in enzymology.

Conclusions. The essential nature of pantothenate biosynthesis in *Mycobacterium tuberculosis*, and the lack of these enzymes in mammals, suggests that enzymes involved in pantothenate biosynthesis would be appropriate targets for inhibitor design or selection. The relatively unique reaction catalyzed by pantothenate synthesase, the ATP-dependent formation of the β-alanyl amide bond of pantothenate, suggests that selective inhibition of this enzyme could be achieved. These studies have revealed not only that a pantoyl adenylate intermediate formed, but also that the rate of its formation and decomposition is sufficiently fast to account for steady-state turnover. Modeling of ATP and pantoate into the unliganded structure of the *E. coli* pantothenate synthetase reveals a number of potential catalytic residues that may be involved in the formation of the pantoyl adenylate intermediate (*11*). The subsequent nucleophilic attack by β-alanine on the adenylate suggests that a tripartite inhibitor, consisting of pantoate, AMP, and β-alanine, would be accommodated in the active site. The ability of the enzyme to catalyze the AMP-dependent cleavage of the peptide bond of pantothenate may be useful in the preparation of pantothenate analogues.

ACKNOWLEDGMENT

We are grateful to Drs. Argyrides Argyrou and Luiz A. Basso for helpful suggestions.

REFERENCES

1. Neidhardt, F. (1996) *Escherichia coli and Salmonella typhimurium*: *cellular and molecular biology*, 2nd ed., Vol. 1, pp 687−694, American Society for Microbiology, Washington, DC.
2. Abiko, Y. (1975) Metabolism of coenzyme A. in *Metabolic Pathways* (Greenburg, D. M., Ed.) Academic Press, Inc., New York.
3. Prescott, D. J., and Vagelos, P. R. (1972) *Adv. Enzymol. Relat. Areas Mol. Biol. 36*, 269−311.
4. Maas, W. K., and Vogel, H. J. (1953) *J. Bacteriol. 65*, 388−393.
5. Brown, G. M., and Williamson, J. M. (1982) *Adv. Enzymol. Relat. Areas Mol. Biol. 53*, 345−381.
6. Cronan, J. E., Jr., Littel, K. J., and Jackowski, S. (1982) *J. Bacteriol. 149*, 916−922.
7. Brown, G. M., and Williamson, J. M. (1987) in *Escherichia coli and Salmonella typhimurium*: *cellular and molecular biology* (Neidhardt, F., Ingraham, J. L., Low, K. B., Magasanik, B., Schaechter, M., and Umbarger, H. E., Eds.) pp 521−538, American Society for Microbiology, Washington, DC.
8. Miyatake, K., Nakano, Y., and Kitaoka, S. (1979) *Methods Enzymol. 62*, 215−219.
9. Miyatake, K., Nakano, Y., and Kitaoka, S. (1978) *J. Nutr. Sci. Vitaminol. 24*, 243−253.
10. Genschel, U., Powell, C. A., Abell, C., and Smith, A. G. (1999) *Biochem. J. 341*, 669−678.
11. von Delft, F., Lewendon, A., Dhanaraj, V., Blundell, T. L., Abell, C., and Smith, A. G. (2001) *Structure 9*, 439−450.
12. Kim, Y. S., and Kang, S. W. (1994) *Biochem. J. 297*, 327−333.
13. Kisselev, L. L., and Favorova, O. O. (1974) *Adv. Enzymol. Relat. Areas Mol. Biol. 40*, 141−238.
14. Papas, T. S., and Peterkofsky, A. (1972) *Biochemistry 11*, 4602−4608.
15. Thiebe, R. (1983) *Eur. J. Biochem. 130*, 517−524.
16. King, H. L., Jr., Dyar, R. E., and Wilken, D. R. (1974) *J. Biol. Chem. 249*, 4689−4695.
17. Laemmli, U. K. (1970) *Nature 227*, 680−685.
18. Pfleiderer, G., Kreiling, A., and Wieland, T. (1960) *Biochem. Z. 333*, 302−307.
19. Cleland, W. W. (1979) *Methods Enzymol. 63*, 103−138.
20. Fersht, A. (1999) *Structure and Mechanism in Protein Science*, 2nd ed., W. H. Freeman, New York.
21. Johnson, K. A. (1992) *Enzymes (3rd Ed.) 20*, 1−60.
22. Segel, I. H. (1975) *Enzyme Kinetics*, p 860, John Wiley & Sons, Inc., New York.
23. Black, P. N., DiRusso, C. C., Sherin, D., MacColl, R., Knudsen, J., and Weimar, J. D. (2000) *J. Biol. Chem. 275*, 38547−38553.
24. Papas, T., and Mehler, A. H. (1971) *J. Biol. Chem. 246*, 5924.
25. Allende, C. C., Chaimovich, H., Gatica, M., and Allende, J. E. (1970) *J. Biol. Chem. 245*, 93.
26. Freist, W., Sternbach, H., and Cramer, F. (1981) *Eur. J. Biochem. 119*, 477−482.
27. Cohn, M., and Hu, A. (1978) *Proc. Natl. Acad. Sci. U.S.A. 75*, 200−203.
28. Wieland, T., Lowe, W., Kreiling, A., and Pfleiderer, G. (1963) *Biochem. Z. 339*, 1−7.
29. Fersht, A. R. (1987) *Biochemistry 26*, 8031−8037.
30. Lessard, I. A. D., Healy, V. L., Park, I. S., and Walsh, C. T. (1999) *Biochemistry 38*, 14006−14022.
31. Ghose, C., and Raushel, F. M. (1985) *Biochemistry 24*, 5894−5898.
32. Eldred, E. W., and Schimmel, P. R. (1972) *Biochemistry 11*, 17.
33. Mullins, L. S., Zawadzke, L. E., Walsh, C. T., and Raushel, F. M. (1990) *J. Biol. Chem. 265*, 8993−8998.

BI011522+